Evaluation of Transient Motion During Gadoxetic Acid–Enhanced Multiphasic Liver Magnetic Resonance Imaging Using Free-Breathing Golden-Angle Radial Sparse Parallel Magnetic Resonance Imaging

Jeong Hee Yoon, MD,† Jeong Min Lee, MD,*†‡ Mi Hye Yu, MD,§ Bo Yun Hur, MD,|| Robert Grimm, PhD,¶ Kai Tobias Block, PhD,#**†† Hersh Chandarana, MD,#**†† Berthold Kiefer, PhD,¶ and Yohan Son, PhD‡‡*

Objectives: The aims of this study were to observe the pattern of transient motion after gadoxetic acid administration including incidence, onset, and duration, and to evaluate the clinical feasibility of free-breathing gadoxetic acid–enhanced liver magnetic resonance imaging using golden-angle radial sparse parallel (GRASP) imaging with respiratory gating.

Materials and Methods: In this institutional review board–approved prospective study, 59 patients who provided informed consents were analyzed. Free-breathing dynamic T1-weighted images (T1WIs) were obtained using GRASP at 3 T after a standard dose of gadoxetic acid (0.025 mmol/kg) administration at a rate of 1 mL/s, and development of transient motion was monitored, which is defined as a distinctive respiratory frequency alteration of the self-gating MR signals. Early arterial, late arterial, and portal venous phases retrospectively reconstructed with and without respiratory gating and with different temporal resolutions (nongated 13.3-second, gated 13.3-second, gated 6-second T1WI) were evaluated for image quality and motion artifacts. Diagnostic performance in detecting focal liver lesions was compared among the 3 data sets.

Results: Transient motion (mean duration, 21.5 ± 13.0 seconds) was observed in 40.0% (23/59) of patients, 73.9% (17/23) of which developed within 15 seconds after gadoxetic acid administration. On late arterial phase, motion artifacts were significantly reduced on gated 13.3-second and 6-second T1WI (3.64 ± 0.34, 3.61 ± 0.36, respectively), compared with nongated 13.3-second T1WI (3.12 ± 0.51, $P < 0.0001$). Overall, image quality was the highest on gated 13.3-second T1WI (3.76 ± 0.39) followed by gated 6-second and nongated 13.3-second T1WI (3.39 ± 0.55, 2.57 ± 0.57, $P < 0.0001$). Only gated 6-second T1WI showed significantly higher detection performance than nongated 13.3-second T1WI (figure of merit, 0.69 [0.63–0.76]) vs 0.60 [0.56–0.65], $P = 0.004$).

Conclusions: Transient motion developed in 40% (23/59) of patients shortly after gadoxetic acid administration, and gated free-breathing T1WI using GRASP was able to consistently provide acceptable arterial phase imaging in patients who exhibited transient motion.

Received for publication May 25, 2017; and accepted for publication, after revision, July 12, 2017.

From the *Department of Radiology, Seoul National University Hospital; †College of Medicine, Seoul National University; ‡Institute of Radiation Medicine, Seoul National University Medical Research Center; §Department of Radiology, Konkuk University School of Medicine, Seoul; ||Department of Radiology, National Cancer Center Korea, Goyang, Republic of Korea; ¶Siemens Healthcare Gmbh, Erlangen, Germany; #Center for Advanced Imaging Innovation and Research (CAI^{2}R); **Bernard and Irene Schwartz Center for Biomedical Imaging; ††Department of Radiology, New York University School of Medicine, New York, NY; and ‡‡Siemens Healthcare Korea, Seoul, Republic of Korea.

Correspondence to: Jeong Min Lee, MD, Department of Radiology, Seoul National University Hospital, 101 Daehak-ro, Jongno-gu, Seoul 03080, Republic of Korea. E-mail: JMSH@SNU.AC.KR; jmlshy2000@gmail.com.

Supplemental digital contents are available for this article. Direct URL citations appear in the printed text and are provided in the HTML and PDF versions of this article on the journal's Web site (www.investigativeradiology.com).

ISSN: 0020-9996/17/0000–0000
DOI: 10.1097/RLI.0000000000000409

Key Words: gadoxetic acid, transient motion, liver, MRI, free breathing, T1WI, GRASP

(*Invest Radiol* 2017;00: 00–00)

Gadoxetic acid-enhanced magnetic resonance imaging (MRI) has been shown to improve the detection and characterization of focal liver lesions (FLLs).[1,2] However, the difficulty of repeated and relatively long breath-holds required for abdominal MRI has led to reduced patient compliance[3] and frequent re-examinations owing to the considerable occurrence of motion artifacts.[4] In addition, the use of gadoxetic acid itself has been reported to result in degraded arterial phase images compared with that using extracellular contrast media, thereby hindering accurate lesion characterization.[5–7] Until now, there have been ample reports documenting "transient dyspnea" or "transient severe motion" frequently occurring after gadoxetic acid administration, although the specific mechanism is not yet fully understood. However, recent studies have shown that the reported incidence based on retrospective image reviews or subjective symptoms[5,6,8] may not reflect the actual incidence.[4,9] Furthermore, although it is known that gadoxetic acid administration can reduce maximal breath-holding duration,[9,10] we do not yet know whether it develops spontaneously without the requirement of a breath-hold. Moreover, if it does develop, we do not know the pattern and duration of transient motion without intervention (breath-holding), which may improve our understanding the relationship between transient motion and subjective symptoms or the degree of image degradation. Until recently, these issues could not be addressed as it was not possible to investigate the development of transient motion, considering the breath-hold requirements to obtain adequate image quality in dynamic T1-weighted imaging (T1WI).

Lately, a free-breathing imaging technique combining incoherent undersampling and parallel imaging with golden-angle radial stack-of-stars sampling (golden-angle radial sparse parallel MRI, GRASP)[11] has been reported to provide free-breathing dynamic T1WI with acceptable image quality.[12] Furthermore, using this sequence, a respiration self-gating signal can be extracted from raw measurement data, and respiratory gating can be performed retrospectively, since the k-space center is read out with every spoke.[13,14] Thus, dynamic T1WI using this sequence may finally allow the evaluation of the characteristics of spontaneous transient motion after gadoxetic acid administration as well as the investigation of the relationship between motion and image quality.

Therefore, the aims of this study are to observe the pattern of transient motion after gadoxetic acid administration including incidence, onset, and duration, and to evaluate the clinical feasibility of free-breathing gadoxetic acid-enhanced liver MRI using GRASP with respiratory gating.

MATERIALS AND METHODS

Financial support for this study was provided by Bayer Healthcare (Berlin, Germany). Three employees of Siemens Healthcare

(R.G., Y.S., and B.K.) also provided technical support for the implementation and optimization of the prototypical pulse sequence, gated GRASP reconstruction, and extraction of the respiratory pattern from MR data. However, authors not associated with Siemens Healthcare (J.H.Y., M.H.Y., B.Y.H., K.B, H.C., and J.M.L.) maintained full control of the data at all times.

Patient Enrollment

This prospective study was performed after approval by the Institutional Review Board of Seoul National University Hospital and registration in the clinicaltrials.gov database (NCT02395991). Written informed consents were obtained from all patients. From April 2015 to October 2015, 60 patients (male-female ratio, 35:25; mean age, 60.1 ± 11.3 years [range, 19–78 years]) were prospectively enrolled according to the following eligibility criteria: (*a*) patients who were scheduled for gadoxetic acid–enhanced liver MRI for FLL characterization or suspicion of diffuse liver disease or (*b*) living liver donor candidates. Exclusion criteria were as follows: (*a*) patients younger than 18 years of age, (*b*) patients with contraindications to contrast-enhanced MRI, or (*c*) patients with biliary obstruction. After MRI, all patients were requested to fill out a questionnaire on subjective symptoms during contrast media administration, which is described in greater detail later. Among the 60 patients, 1 patient without subjective symptoms was excluded due to raw data storage failure for extraction of the respiratory curve and additional retrospective image reconstruction. Thus, analyses of the breathing patterns and image quality were performed for the remaining 59 patients (male-female ratio, 34:25; mean age, 58.9 ± 11.7 years in men [range, 19–78] and 61.4 ± 10.9 years in women [range, 25–76]). Underlying disease and laboratory findings including albumin, total bilirubin, prothrombin time, and creatinine were recorded.

MRI Acquisition

All examinations were performed at a 3 T MR unit (MAGNETOM Skyra; Siemens Healthcare, Erlangen, Germany) using a standard 48-channel phased array body coil. The MR examination consisted of precontrast heavily T2-weighted images (T2WIs), diffusion-weighted images using 2 *b*-values (0, 800 s/mm^2), dual-echo precontrast T1WI, precontrast T1WI, dynamic T1WI, and the hepatobiliary phase (HBP) images. Dynamic T1WI was obtained using the prototype GRASP implementation. Precontrast T1WI and HBP images were each obtained using a conventional breath-hold 3-dimensional gradient echo sequence and the GRASP technique, respectively. Detailed scan parameters are shown in Supplemental Digital Content 1, Table 1E, http://links.lww.com/RLI/A342.

Free-Breathing T1WI Acquisition Using GRASP

As previously described in the literature,[12] the GRASP technique is based on a stack-of-stars 3-dimensional spoiled gradient-recalled echo pulse sequence with fat suppression and golden-angle radial sampling, followed by a compressed sensing reconstruction with through-time total variation regularization. This technique also allows for retrospective respiratory gating based on a self-gating signal that can be derived from the signal variations at the k-space center.[14] For each patient, 4 separate GRASP acquisitions were performed:

For the first scan, patients were requested to hold their breath for as long as possible in expiration, up to 60 seconds, to check their maximum breathing capacity before saline injection. A total number of 406 radial spokes was acquired over 60 seconds. The images were not further analyzed, but only the respiratory self-gating signal was extracted from the raw k-space data. The breath-hold capacity was determined as the interval between scan initiation and the first detected motion according to the self-gating signal, and patients with less than 10 seconds were classified as those with short breath-holding capability.

Second, precontrast T1WI was obtained for 90 seconds (609 radial spokes) with the second GRASP scan during free breathing and intravenous saline injection, using the same injection volume as for the later injection of gadoxetic acid, and at a rate of 1.0 mL/s. This procedure was part of the routine process to check the patency of the intravenous route before contrast media injection. The self-gating signal was extracted, representing regular breathing before contrast medium injection. The extracted respiratory signals also served as a control to determine transient motion after contrast media administration.

Third, dynamic T1WI using the GRASP technique was obtained continuously during free breathing for 3 minutes and 30 seconds (1620 radial spokes). The scan was performed during simultaneous injection of a standard dose of gadoxetic acid (0.025 mmol/kg, Primovist or Eovist; Bayer Healthcare, Berlin, Germany) administered at a rate of 1.0 mL/s followed by a 20-mL saline chaser, without a fixed time delay or bolus tracking. Again, the corresponding respiratory self-gating signal was extracted and analyzed to detect changes in the patients' breathing patterns during the contrast agent administration.

Fourth and lastly, the HBP was obtained 15 minutes after contrast media injection using the GRASP sequence for 60 seconds (406 radial spokes). During the scan, patients were requested to relax and breathe comfortably.

GRASP Image Reconstruction

As mentioned previously, precontrast T1WI during the breath-hold capacity scan was discarded. Precontrast T1W during saline injection and dynamic T1W images were reconstructed off-line with and without respiratory gating[14] using 89 spokes, which corresponds to a temporal resolution of 13.3 seconds. In addition, one more retrospective, respiratory-gated reconstruction using 42 spokes, corresponding to a temporal resolution of 6 seconds, was performed. Hepatobiliary phase images were also reconstructed off-line with 89 spokes (13.3 seconds) and respiratory gating. Besides, dynamic T1WI was additionally reconstructed using automatic bolus detection function described in a previous study,[15] which only served as a guidance to choose 1 early arterial, late arterial, and portal venous phases for review among multiple arterial and portal venous phases.

Patient Monitoring

During the examinations, patients were monitored by 1 experienced nurse and a radiology technician. Patients' heart rate and oxygen saturation were also recorded before contrast media injection; at the time of saline injection; at the time of contrast media injection; and at 10 seconds, 30 seconds, 60 seconds, and 180 seconds after contrast media administration. The highest value of the heart rate and lowest value of oxygen saturation (SpO_2) between each time point was chosen as the representative value of each time point. Intravenous administration of saline and gadoxetic acid was notified to patients as in a clinical routine, but the type of media (saline or gadoxetic acid) was not specified at the time of administration.

Subjective symptoms were reported by checking the questionnaire after MRI. The questionnaire included various potential adverse effects from none to nausea, vomiting, dyspnea, and other sensations, and patients were allowed to check among a binary response (yes or no). If patients experienced other symptoms, it was requested to be specified in a descriptive manner.

Image Analysis

Image Quality Assessment

One experienced radiologist (J.M.L.) chose the early arterial, late arterial, and portal venous phases among the reconstructed series. Three fellowship-trained abdominal radiologists (J.H.Y., M.H.Y., and B.Y.H.) reviewed the images independently in the order of gated 13.3-second time resolution images, nongated 13.3-second time resolution images,

and gated 6-second temporal resolution images with longer than 2-week intervals between review sessions. Adequacy of arterial phase timing was assessed on a 5-point scale as follows: 1 = early arterial (contrast material in the hepatic artery but no portal vein or parenchymal enhancement), 2–4 = adequate late arterial (2, faint portal vein opacification; 3, portal vein opacification with minimal or mild parenchymal enhancement; and 4, portal vein opacification with definite parenchymal enhancement, but no hepatic venous enhancement), and 5 = too late (strong parenchymal enhancement or hepatic venous enhancement). Motion and streak artifacts were assessed on a 4-point scale as follows: 1 = severe artifacts hindering diagnostic capability of the readers, 2 = moderate artifacts with image quality decrease but no diagnostic performance impairment, 3 = mild artifacts without significant image quality disturbance, and 4 = no perceivable artifacts. Liver edge sharpness was scored on a 4-point scale: score 1 (extreme blur), 2 (partially indistinctive liver margin with moderate blur), 3 (slightly soft liver margin with mild blur), and 4 (clear liver margin and minimal blur). Overall image quality was also graded on a 4-point scale as follows: 1 = nondiagnostic, 2 = not satisfactory image quality but re-examination not required, 3 = acceptable image quality, and 4 = comparable with average breath-hold image quality. For the early or late arterial phase, optimal arterial phase acquisition was determined per patient as when the arterial timing was between 2 and 4, and overall image quality was 3 or higher.

Presence of Transient Motion

Respiration curves were extracted from the MR raw data of the dynamic T1WI measurement data of each patient.[14] Transient motion was defined as a distinctive temporary frequency alteration, longer than 1 breathing cycle, of the extracted breathing curve occurring after contrast media administration based on our prior knowledge of transient dyspnea.[5,6] Two radiologists (J.H.Y., J.M.L.) who were blinded to patients' vital sign and subjective symptoms analyzed the extracted data after saline and gadoxetic acid administration in consensus.

Focal Liver Lesion Identification

Based on precontrast, early arterial, late arterial, and portal venous phases, reviewers were requested to identify FLLs in each patient, if any exist. Size, segment, presence or enhancement, and readers' confidence were recorded for the identified FLLs. The presence of enhancement was assessed by comparing precontrast, early arterial, and late arterial phases. Diagnostic confidence was scaled on a 5-point scale as follows: 1 = definitely pseudolesion; 2 = probably pseudolesion; 3 = indeterminate; 4 = probably true lesion; and 5 = definitely true lesion. Then, FLLs were identified on HBP images using the gated GRASP and breath-hold technique. The presence and characterization of FLLs were determined based on breath-hold HBP images with a flip angle of 30 degrees in addition to all acquired MR images, and previous and follow-up images by one radiologist (J.M.L.) who did not participate in the image review.

Standard of Reference for FLLs

A total of 270 FLLs in 55 patients were identified; the characteristics of FLLs are summarized in the Appendix (Supplemental Digital Content 2, Table E2, http://links.lww.com/RLI/A343). Metastasis, focal fat deposition, and eosinophil abscess were histologically confirmed. Diagnosis of posttreatment lesions (percutaneous ethanol injection, radiofrequency ablation, transarterial chemoembolization) was made based on treatment history and previous images. Hepatic cysts, hemangiomas, and FNH-like nodules were diagnosed according to characteristic imaging features as described in previous studies[16–18] and follow-up images with at least a 6-month interval. Dysplastic nodules (DNs) were defined as variable size nonhypervascular nodules showing HBP hypointensity, but no interval growth over 6 months or other ancillary features of malignancy such as diffusion restriction or T2 intermediate hyperintensity.[19,20] Twenty-one HCCs were diagnosed histologically (n = 11; 17.1 ± 10.9 mm; range, 5–37 mm) or based on imaging features according to LI-RADS[21,22]

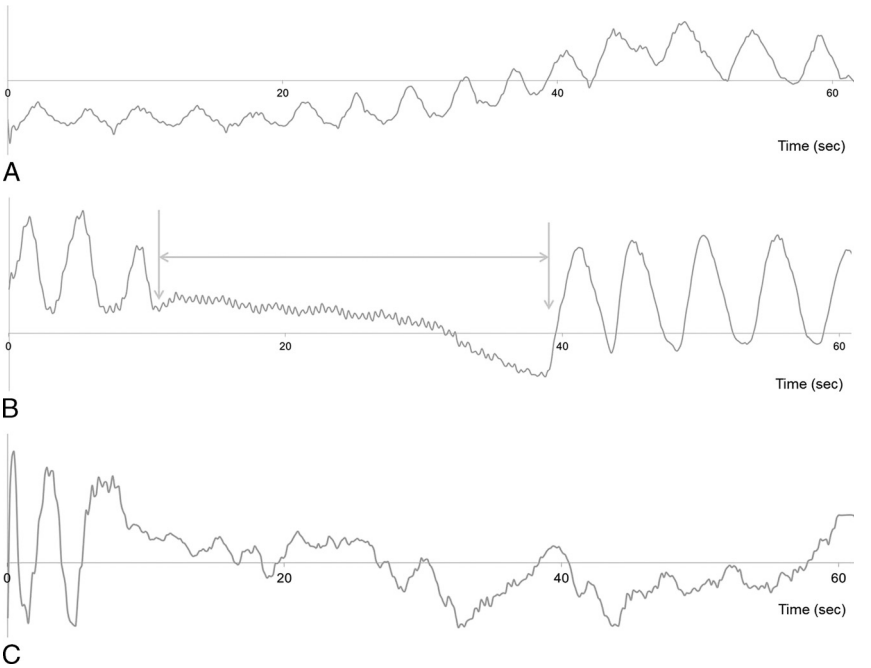

FIGURE 1. Respiratory motion curves (self-gating signal) of different breathing patterns on dynamic T1WI. The *x* axis indicates the time (second), and the *y* axis is unitless. Scan was done with GRASP simultaneously with gadoxetic acid administration at time point zero. A, Respiratory curve showing a normal breathing rhythm without transient motion in a 71-year-old man without any subjective symptoms. B, Alteration of respiratory motion frequency was observed for 27.1 seconds (from 10.5–37.6 seconds after gadoxetic acid administration) in a 51-year-old man and was regarded as transient motion (arrows). The patient had neither alteration of vital signs nor subjective symptoms. C, Respiratory graph showing an irregular breathing pattern in a 75-year-old woman with liver cirrhosis. Figure 1 can be viewed online in color at www.investigativeradiology.com.

as follows: LR-5 or LR-5 V on prior computed tomography by within 6 weeks (n = 10; 46.0 ± 67.1 mm; range, 10–187 mm). In addition, we considered 10 LR-4 nodules (11.8 ± 4.4 mm; range, 7–21 mm) as being HCCs, which showed all of the following features: (*a*) tumor staining and lipiodol uptake on follow-up transarterial chemoembolization, (*b*) more than 2 ancillary features on the nondynamic phase of MRI (diffusion restriction, HBP hypointensity, T2 intermediate hyperintensity), and (*c*) patients with a history of HCC. Cirrhotic nodules were defined as distinctive nodules on the HBP images with or without iron deposition that did not satisfy the criteria of DN or HCC in addition to being stable on follow-up images. In 4 patients, the absence of FLL was confirmed on follow-up images after 6 to 12 months.

Statistical Analysis

Reader scores were averaged and continuous variables including readers score were presented in mean ± standard deviation along with range. Imaging scores were analyzed using the paired *t* test between 2 images with different time resolutions or respiratory gating. Interrater agreement was assessed using an average-measure 2-way random-effects intraclass correlation coefficient (ICC) for qualitative analysis regarding image quality.[23] The ICC of interobserver agreement was assessed as poor (<0.40), fair to good (0.40–0.75), or excellent (>0.75).[10] Categorical variables were analyzed using the χ^2 test or Fisher exact test between patients with and without transient motion. In addition, changes in SpO_2 and heart rate were compared between groups with and without transient motion during the scan time using Student *t* test. Substantial decrease in oxygen saturation was defined as a decrease of 4 or more percentage compared with that before contrast media administration.[9]

For analysis of the diagnostic performance of MR sequences in the detection of FLLs, jackknife alternative free-response receiver operating characteristic (JAFROC) analysis was performed using noncommercial software (JAFROC, version 4.2.1; http://www.devchakraborty.com).[24] Average diagnostic accuracy was obtained using the mean figure of merit (FOM) defined as the probability that the rating of the highest-rated lesion with correct localization and diagnosis exceeds that of the highest-rated nonlocalization mark in a normal case,[25] and calculated based on a fixed reader and random cases. Differences in FOMs between sequences were calculated across readers. For multiple comparisons of dynamic sequences, a Bonferroni-corrected *P* value was used to indicate statistical significance. Other statistical analyses were performed using commercially available software (MedCalc, version 12; MedCalc Software, Mariakerke, Belgium and IBM SPSS Statistics, version 22.0; SPSS Inc, Armonk, NY). A *P* value less than 0.05 ($P < 0.017$ in 3 comparisons after Bonferroni correction) was considered to indicate a statistically significant difference.

RESULTS

Breath-Holding Capacity, Respiratory Pattern, and Incidence of Transient Respiratory Motion

In the 59 patients in our study, mean breath-holding capacity was 33.4 ± 17.3 seconds (range, 2.3–60.0). There were 6 patients with breath-holding capability less than 10 seconds (6.1 ± 2.5; range, 2.3–10.0). According to breathing-pattern monitoring based on the extracted self-gating signals, transient motion was observed in 40.0% (23/59) of patients after gadoxetic acid injection, 0% (0/59) of patients after saline injection, and presence of transient motion was not assessed

TABLE 1. Characteristics of Patients

	Nontransient Motion Group (n = 35)	Transient Motion Group (n = 23)	Severely Irregular Breathing (n = 1)	*P*
Sex (male-female ratio)	20:15	14:9	0:1	0.99
Age, y	58.9 ± 10.2 (25–75)	60.9 ± 13.0 (19–78)	75	0.20
Amount of gadoxetic acid, mL	6.2 ± 0.8 (4.7–8.4)	6.6 ± 1.1 (4.6–8.5)	4.4	0.22
Breath-holding capacity, s	30.8 ± 18.1 (2.3–60.0)	37.4 ± 16.1 (10.0–60.0)	29.9	0.17
Subjective symptoms				
No	82.9% (29/35)	87% (20/23)	100% (1/1)	0.96
Yes	17.1% (6/35)	13.0% (3/23)	0% (0/1)	
Nausea	2.9% (1/35)	8.7% (2/23)	0% (0/1)	
Dyspnea	2.9% (1/35)	0% (0/23)	0% (0/1)	
Dyspnea and warm sensation at the arm	2.9% (1/35)	0% (0/23)	0% (0/1)	
Itching sense	5.7% (2/35)	0% (0/23)	0% (0/1)	
Abdominal rigidity	0% (0/35)	4.3% (1/23)	0% (0/1)	
Irritation at the injection site	2.9% (1/35)	0% (0/23)	0% (0/1)	
Underlying disease				
Coronary artery disease	11.4% (4/35)	0% (0/23)	0% (0/1)	0.25
Asthma	0% (0/35)	0% (0/23)	0% (0/1)	0.15
Tuberculosis	11.4% (4/35)	0% (0/23)	0% (0/0)	0.25
COPD	2.9% (1/35)	0% (0/23)	0% (0/1)	0.83
Laboratory finding				
Albumin, g/dL	4.1 ± 0.5 (2.5–4.7)	4.0 ± 0.4 (3.1–4.6)	3.8	0.30
Total bilirubin, mg/dL	1.3 ± 2.2 (0.4–13.9)	1.1 ± 0.6 (0.4–2.6)	0.9	0.87
Prothrombin time, INR	1.1 ± 0.2 (0.9–2.0)	1.1 ± 0.1 (0.9–1.4)	1.1	0.48
Creatinine, mg/dL	0.8 ± 0.2 (0.6–1.2)	0.9 ± 0.2 (0.6–1.5)	0.7	0.34

Values are mean ± standard deviation (range). $P < 0.05$ indicates statistically significant difference between groups with and without transient motion. COPD, chronic obstructive pulmonary disease.

due to persistent irregular breathing in 1 patient (1.7% [1/59]) after both saline and gadoxetic acid administration. Transient motion after gadoxetic acid administration lasted for 21.5 ± 13.0 seconds on average (range, 5.0–52.4 seconds), and the onset time of transient motion was 10.4 ± 12.6 seconds (range, 0.05–39.8 seconds) after contrast media injection (Fig. 1). In 87.0% (20/23) of patients with transient motion, motion developed within 30 seconds, and 73.9% (17/23) of patients showed transient motion within 15 seconds after contrast media administration.

Signs and Symptoms During Continuous Acquisition of GRASP

During acquisition of dynamic T1WI using the GRASP sequence for 3 minutes and 30 seconds, SpO_2 and heart rate of the study patients were monitored. There were no significant differences in SpO_2 and heart rate between nontransient motion and transient motion groups across all time points (P = 0.25–0.99, Supplemental Digital Content 3, Table E3, http://links.lww.com/RLI/A344). There were no patients with a substantial SpO_2 decrease after contrast media administration. The prevalence of subjective symptoms did not show a significant difference between groups with and without transient motion (13.0% [3/23] vs 17.1% [6/35], P = 0.96; Table 1). In addition, there were no significant differences in potentially motion-associated subjective symptoms such as dyspnea or nausea between the 2 groups (8.7% [2/23] vs 8.6% [3/35], P = 0.64; Table 1).

Image Quality Assessment of Free-Breathing T1WI Using GRASP

Dynamic T1WI was successfully obtained using the GRASP technique in all patients. Qualitative analysis results of nongated 13.3-second, gated 13.3-second, and gated 6-second T1WI are summarized in Table 2.

Overall Image Quality

On late arterial phase, gated 13.3-second GRASP images (Fig. 2) and gated 6-second GRASP images showed significantly better image quality than nongated 13.3-second GRASP images (3.76 ± 0.39, 3.39 ± 0.55 vs 2.57 ± 0.57, P < 0.0001), as well as on early arterial and portal venous phases (Table 2, P < 0.0001 in all). In the comparison of gated 13.3-second and 6-second images, overall image quality and liver edge sharpness of gated 13.3-second T1WI was significantly better than gated 6-second T1WI in all dynamic phases (Table 2, P < 0.0001 in all).

Image Artifacts in 3 Reconstructed Dynamic T1WI

Among the 3 reconstructed GRASP images, motion artifacts were the most substantial on nongated 13.3-second T1WI, and motion artifact was significantly reduced on gated 13.3-second and gated 6-second T1WI on late arterial phase (3.12 ± 0.51 vs 3.64 ± 0.34, 3.61 ± 0.36, P < 0.0001), as well as on early arterial and portal venous phases (Table 2, P < 0.0001). There were no significant differences in motion artifacts between gated 13.3-second and 6-second T1WI during all phases (Table 2, P = 0.07–0.24). As for streak artifacts, gated 13.3-second T1WI showed a higher score than nongated 13.3-second T1WI in all dynamic phases (P < 0.0001), and gated 6-second T1WI showed higher streak artifacts than gated 13.3-second T1WI on all phases (P < 0.0001; Table 2).

Acquisition of the Optimal Timing of the Late Arterial Phase

On gated 13.3-second and 6-second GRASP images, all 59 patients (100%) obtained at least 1 optimal late arterial phase timing (timing 2 to 4), whereas 1 patient obtained only too early phase on nongated 13.3-second GRASP images. On basis of timing and image quality, late arterial phase with unacceptable image quality (<2) or missed timing (timing <2 or >4) were observed in 5.1% (3/59), 0% (0/59), and

TABLE 2. Qualitative Analysis of Image Quality of Dynamic T1WI With and Without Respiratory Gating and Variable Temporal Resolution

	Sequence			*P*		
	Nongated 13.3-s (A)	**Gated 13.3-s (B)**	**Gated 6-s (C)**	**A vs B**	**A vs C**	**B vs C**
EAP						
Timing	1.54 ± 0.58 (1.0–3.0)	1.54 ± 0.52 (1.0–2.7)	1.73 ± 0.36 (1.0–2.3)	0.912	0.019	0.009
Motion artifact	3.12 ± 0.46 (2.0–4.0)	3.64 ± 0.40 (1.7–4.0)	3.59 ± 0.37 (2.3–4.0)	<0.0001	<0.0001	0.20
Streak artifact	3.27 ± 0.41 (2.3–4.0)	2.88 ± 0.36 (2.0–3.7)	2.74 ± 0.47 (2.0–4.0)	<0.0001	<0.0001	0.016
Liver edge sharpness	2.28 ± 0.44 (1.3–3.7)	3.52 ± 0.64 (1.7–4.0)	3.39 ± 0.61 (1.7–4.0)	<0.0001	<0.0001	0.001
Overall image quality	2.58 ± 0.45 (1.0–3.7)	3.64 ± 0.53 (2.0–4.0)	3.32 ± 0.62 (1.7–4.0)	<0.0001	<0.0001	<0.0001
LAP						
Timing	3.27 ± 0.65 (1.7–5.0)	3.33 ± 0.42 (2.0–4.0)	3.07 ± 0.21 (2.7–3.7)	0.47	0.021	<0.0001
Motion artifact	3.12 ± 0.51 (1.7–4.0)	3.64 ± 0.34 (2.3–3.3)	3.61 ± 0.36 (2.3–4.0)	<0.0001	<0.0001	0.24
Streak artifact	3.31 ± 0.42 (2.3–4.0)	3.02 ± 0.35 (2.0–3.7)	2.85 ± 0.43 (2.0–3.7)	<0.0001	<0.0001	0.003
Liver edge sharpness	2.24 ± 0.46 (1.0–3.7)	3.61 ± 0.54 (2.0–4.0)	3.38 ± 0.56 (1.7–4.0)	<0.0001	<0.0001	<0.0001
Overall image quality	2.57 ± 0.57 (1.0–3.7)	3.76 ± 0.39 (2.7–4.0)	3.39 ± 0.55 (1.7–4.0)	<0.0001	<0.0001	<0.0001
PVP						
Timing	4.78 ± 0.33 (4.3–5.0)	4.88 ± 0.18 (4.3–5.0)	4.94 ± 0.12 (4.7–5.0)	0.53	0.001	0.003
Motion artifact	3.20 ± 0.53 (2.0–4.0)	3.8 ± 0.28 (2.3–4.0)	3.74 ± 0.20 (3.0–4.0)	<0.0001	<0.0001	0.07
Streak artifact	3.47 ± 0.37 (2.3–4.0)	3.39 ± 0.38 (2.3–4.0)	3.21 ± 0.41 (2.3–2.7)	<0.0001	<0.0001	<0.0001
Liver edge sharpness	2.33 ± 0.46 (1.3–3.7)	3.78 ± 0.37 (2.7–4.0)	3.75 ± 0.34 (2.7–4.0)	<0.0001	<0.0001	0.54
Overall image quality	2.79 ± 0.48 (1.7–3.7)	3.91 ± 0.24 (3.0–4.0)	3.59 ± 0.47 (2.0–4.0)	<0.0001	<0.0001	<0.0001

Values are mean ± SD (range). P < 0.017 was statistically significant. T1WI indicates T1-weighted image; EAP, early arterial phase; LAP, late arterial phase; PVP, portal venous phase.

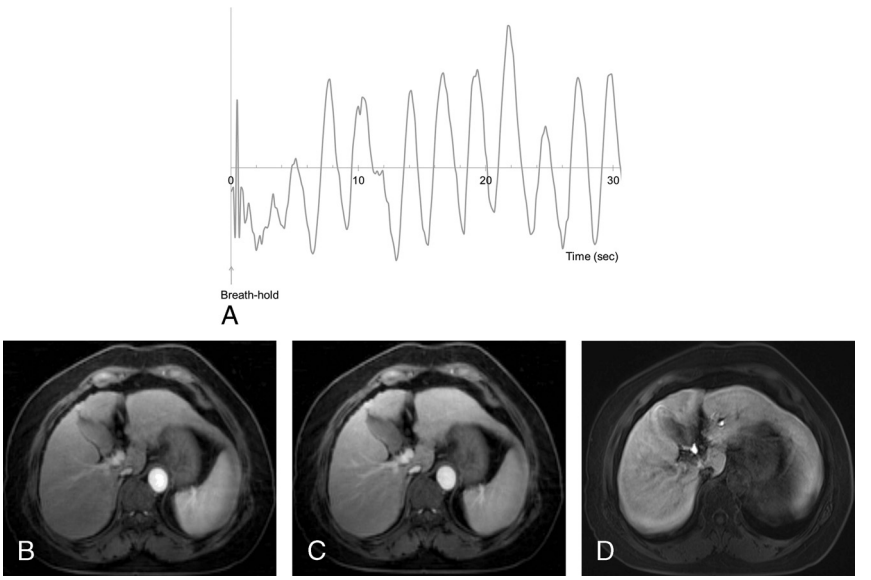

FIGURE 2. Feasibility of respiratory-gated free-breathing T1WI. A 67-year-old woman with liver cirrhosis showed limited breath-hold capacity of less than 5 seconds on the precontrast breath-holding capacity test (A). Gated 13.3-second T1WI with 3-mm slice thickness showed acceptable arterial phase (B) and portal venous phase (C) images without significant motion artifact, whereas motion artifact and image blur were observed on 4-mm thickness breath-hold T1WI of the hepatobiliary phase (D). Figure 2 can be viewed online in color at www.investigativeradiology.com.

1.7% (1/59) on nongated 13.3-second, gated 13.3-second, and gated 6-second images.

Comparison of Image Quality of GRASP Images in Patients With and Without Transient Respiratory Motion

On nongated 13.3-second T1WI, motion artifacts were significantly greater in patients with transient motion (Table 3, $P = 0.001$–0.005), and image quality was significantly lower in the early arterial and late arterial phases than in patients without transient motion (Table 3, $P = 0.003$ and 0.005). Compared with nongated 13.3-second late arterial phase, 24 patients with transient motion (n = 23) or severely irregular breathing (n = 1) showed significantly decreased motion artifacts after respiratory gating: 2.85 ± 0.54 on gated 13.3-second vs 3.57 ± 0.44 on gated 13.3-second ($P < 0.0001$), and 3.5 ± 0.47 on gated 6-second images ($P < 0.0001$; Fig. 3). In these patients, the average score of overall image quality was 3.44 ± 0.70 on the early arterial phase and 3.60 ± 0.49 on the late arterial phase on gated 13.3-second images.

Overall, reader agreement was fair to excellent (ICC = 0.46–0.87), except for motion artifacts on the nongated early arterial phase using a 13.3-second temporal resolution (ICC = 0.37, Supplemental Digital Content 4, Table E4, http://links.lww.com/RLI/A345).

Diagnostic Performance of Dynamic T1WI Using GRASP

Diagnostic performances of free-breathing dynamic T1WI are summarized in Table 4. The reader-averaged values of the FOM of 3 reviewers were 0.60 for nongated 13.3-second T1WI, 0.64 for gated 13.3-second T1WI, and 0.69 for gated 6-second T1WI (Fig. 4). According to the pairwise comparison, gated 6-second T1WI showed significantly higher FOM than nongated 13.3-second T1WI (Table 4, $P = 0.004$). However, there were no significant differences in other pairwise comparisons.

DISCUSSION

In our study, transient respiratory motion spontaneously developed after gadoxetic acid administration in 40.0% (23/59) of the patients under the free-breathing condition. The duration of transient motion was 21.5 ± 13.0 seconds on average (range, 5.0–52.4 seconds) and in 73.9% (17/23) patients, it started within 15 seconds after gadoxetic acid administration. Gadoxetic acid is well known to reduce the breath-hold capability,[9,10,26] and our study showed it also induced involuntary motion under the free-breathing condition. The onset of the transient motion developing shortly after contrast media administration (in 15 seconds) explains its impact on the late arterial phase images as the late arterial scan is often acquired approximately 15 to 20 seconds after contrast administration.[6,26,27] The prevalence of transient motion was shown to be significantly higher with respiratory motion monitoring than the estimation based on the subjective symptom questionnaire (15.3%, 9/59). Indeed, 87% (20/23) of patients with transient motion did not report any symptoms, and we did not find significant changes in oxygen saturation or heart rate during the monitoring either. This finding is consistent with the results of a previous report,[9] and we do not yet know the reason for the lower incidence with self-reporting. However, because the duration varied (5.0–52.4 seconds), we surmise that the patients may not have been aware of the motion or that they may have underrated their experience as it was only transient. Furthermore, the variable duration of transient motion may also explain the variable image quality on affected dynamic phases. Thus, our study suggests that the prevalence of transient motion may be underestimated if it is measured solely based on subjective symptoms or image review. In addition, it could be the reason that the risk factors of transient dyspnea after gadoxetic acid administration may have been inconsistently reported in the literature.[27,28] Since the description of transient motion were reported only in condition of intervention (breath-holding requirement), we believe that our findings of onset and duration may contribute to understanding this phenomenon as well as variable reports in the literature.

We also observed that the GRASP technique allowed diagnostic quality dynamic image acquisition without breath-holding. Especially with respiratory gating, we were able to achieve better image quality and less motion artifacts, compared with non-gated GRASP T1WI, even in patients with transient motion. It indicates that irregular motion is also eliminated well, even without the use of additional navigator signals or external devices. Traditionally, body MRI is performed using rapid imaging sequences in the breath-hold state, and repetitive breath-holds are necessary for dynamic T1WI of liver MR examinations

TABLE 3. Comparison of Qualitative Analysis of Dynamic T1WI With Different Reconstruction Between Patients With and Without Transient Motion

	EAP		LAP		PVP		*P*		
	Nontransient Motion	Transient Motion*	Nontransient Motion	Transient Motion*	Nontransient Motion	Transient Motion*	EAP	LAP	PVP
Nongated 13.3-s									
Timing	1.57 ± 0.65 (1.0–3.0)	1.48 ± 0.49 (1.0–2.3)	3.40 ± 0.72 (1.7–5.0)	3.08 ± 0.48 (2.0–4.0)	4.79 ± 0.34 (4.3–5.0)	4.76 ± 0.32 (4.0–5.0)	0.59	0.064	0.76
Motion artifact	3.29 ± 0.36 (2.7–4.0)	2.87 ± 0.49 (2.0–4.0)	3.31 ± 0.40 (2.3–4.0)	2.85 ± 0.54 (1.7–4.0)	3.35 ± 0.47 (2.3–4.0)	2.97 ± 0.54 (2.0–4.0)	0.001	0.001	0.005
Streak artifact	3.34 ± 0.38 (2.3–2.7)	3.15 ± 0.43 (2.3–4.0)	3.41 ± 0.41 (2.7–4.0)	3.15 ± 0.38 (2.3–3.7)	3.54 ± 0.33 (2.7–4.0)	3.35 ± 0.40 (2.3–4.0)	0.08	0.018	0.033
Liver edge sharpness	2.39 ± 0.46 (2.0–3.7)	2.13 ± 0.35 (1.3–3.0)	2.37 ± 0.44 (2.0–3.7)	2.04 ± 0.44 (1.0–3.0)	2.40 ± 0.49 (1.3–3.7)	2.24 ± 0.39 (1.3–3.0)	0.015	0.007	0.18
Overall image quality	2.73 ± 0.39 (2.0–3.7)	2.38 ± 0.46 (1.0–3.3)	2.73 ± 0.49 (2.0–3.7)	2.32 ± 0.58 (1.0–3.3)	2.90 ± 0.46 (2.0–3.7)	2.63 ± 0.47 (1.7–3.3)	0.003	0.005	0.31
Gated 13.3-s									
Timing	1.55 ± 0.56 (1.0–2.7)	1.54 ± 0.48 (1.0–2.3)	3.31 ± 0.45 (2.0–4.0)	3.37 ± 0.39 (3.0–4.0)	4.87 ± 0.20 (4.3–5.0)	4.9 ± 0.14 (4.7–5.0)	0.94	0.66	0.47
Motion artifact	3.75 ± 0.20 (3.0–4.0)	3.48 ± 0.54 (1.7–4.0)	3.69 ± 0.25 (1.0–2.0)	3.57 ± 0.44 (2.3–4.0)	3.84 ± 0.18 (3.3–4.0)	3.74 ± 0.39 (2.3–4.0)	0.03	0.42	0.18
Streak artifact	2.91 ± 0.34 (2.0–3.7)	2.8 ± 0.38 (2.0–3.7)	3.07 ± 0.30 (2.3–3.3)	2.94 ± 0.41 (2.0–3.7)	3.46 ± 0.35 (2.3–4.0)	3.29 ± 0.39 (2.3–4.0)	0.35	0.15	0.08
Liver edge sharpness	3.67 ± 0.37 (2.7–4.0)	3.31 ± 0.73 (1.7–4.0)	3.73 ± 0.38 (2.7–4.0)	3.42 ± 0.68 (2.0–4.0)	3.8 ± 0.32 (2.7–4.0)	3.7 ± 0.42 (2.7–4.0)	0.23	0.18	0.19
Overall image quality	3.77 ± 0.33 (3.0–4.0)	3.44 ± 0.70 (2.0–4.0)	3.88 ± 0.26 (3.0–4.0)	3.60 ± 0.49 (2.7–4.0)	3.95 ± 0.14 (3.3–4.0)	3.83 ± 0.33 (3.0–4.0)	0.08	0.02	0.25
Gated 6-s									
Timing	1.73 ± 0.34 (1.0–2.3)	1.73 ± 0.38 (1.0–2.0)	3.04 ± 0.21 (2.7–3.7)	3.10 ± 0.20 (2.7–3.7)	4.92 ± 0.13 (4.7–5.0)	4.96 ± 0.10 (4.7–5.0)	0.98	0.24	0.22
Motion artifact	3.7 ± 0.19 (3.0–4.0)	3.43 ± 0.50 (2.3–4.0)	3.68 ± 0.25 (2.7–4.0)	3.5 ± 0.47 (2.3–4.0)	3.78 ± 0.13 (3.7–4.0)	3.7 ± 0.26 (3.0–4.0)	0.024	0.15	0.12
Streak artifact	2.87 ± 0.42 (2.7–3.7)	2.55 ± 0.49 (2.0–3.3)	2.99 ± 0.40 (2.3–3.7)	2.64 ± 0.39 (2.0–3.3)	3.29 ± 0.42 (2.3–4.0)	3.09 ± 0.38 (2.3–3.7)	0.009	0.001	0.15
Liver edge sharpness	3.58 ± 0.42 (2.3–4.0)	3.06 ± 0.72 (1.7–4.0)	3.57 ± 0.36 (2.7–4.0)	3.12 ± 0.70 (1.7–4.0)	3.83 ± 0.29 (2.7–4.0)	3.70 ± 0.42 (2.7–4.0)	0.005	0.016	0.044
Overall image quality	3.49 ± 0.49 (2.3–4.0)	3.06 ± 0.70 (1.7–4.0)	3.54 ± 0.43 (2.3–4.0)	3.19 ± 0.65 (1.7–4.0)	3.70 ± 0.39 (3.0–4.0)	3.44 ± 0.55 (3.0–4.0)	0.007	0.036	0.08

Values are mean ± SD (range). *P* values indicate the difference between groups with and without transient motion on each phase. *One patient with persistent motion was included in this group. T1WI indicates T1-weighted image; EAP, early arterial phase; LAP, late arterial phase; PVP, portal venous phase.

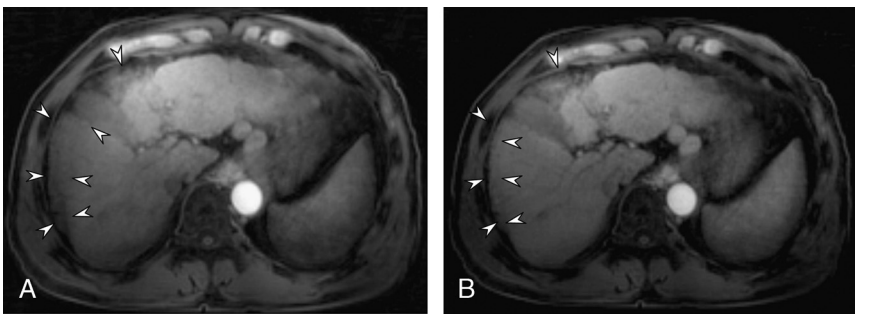

FIGURE 3. Effect of respiratory gating in a 51-year-old patient with transient motion. On late arterial phase without respiratory gating (A), significant motion artifacts and decreased signal in the right lobe due to motion artifact were shown on the late arterial phase (arrowheads). In the respiratory-gated reconstruction, respiratory motion artifacts decreased (arrowheads) and image quality improved (B). The onset and duration of transient motion is provided in Fig. 1B.

using sequences within the Cartesian acquisition scheme.[3,4,27,29,30] Although this allows detailed assessment of various abdominal diseases owing to body MR's high spatial and contrast resolution capability, motion artifacts have been shown to impair the image quality leading to the loss of diagnostic information in uncooperative patients.[4,27] Radial gradient echo sequence sequences, on the other hand, provide a unique approach to this issue by allowing free-breathing dynamic T1WI,[12,31] as the repeated sampling of the k-space center during radial acquisition results in temporal averaging of the information and, thus, reduces sensitivity to motion.[12,32] Our results suggest that GRASP technique allows clinically acceptable quality of free-breathing dynamic T1WI and may improve patients' compliance of abdominal MRI, as previously suggested.[12,32] Although there remains concern that streak artifacts may increase with the undersampled data,[32] the image quality of gated GRASP images was demonstrated to be better than the nongated images in our study. Thus, we believe that the combination of respiratory gating and free-breathing GRASP is preferable, especially for patients who exhibit transient or persistent irregular motion. There is also the possibility that the application of more advanced respiratory motion gating such as motion-resolved reconstruction[33–35] may lead to even better suppression of motion and undersampling artifacts in the near future.

Another finding of our study is that the late arterial phase could be obtained in all patients, demonstrating another benefit of GRASP versus conventional breath-hold approach using fixed delay. Previously, several attempts have been made to attain timely arterial phase images in gadoxetic acid–enhanced liver MRI, and the acquisition of multiphasic arterial phases using short acquisition times[8] or view-sharing techniques[30,36] reduced the risk of missing the optimal arterial timing. However, multiphasic acquisition may require MR fluoroscopic technique for improve yielding of optimal late arterial phase.[30] In addition, it is not able to recover the ruined or missed arterial phase, and the spoiled dynamic phase always necessitated re-examinations. However, GRASP allows a continuous scan and flexible reconstruction that in turn can be retrospectively reconstructed with variable temporal resolution, and the "missed" arterial phase can be recovered by rereconstruction with different temporal resolutions based on the measured raw data as we have shown in this study. Therefore, we believe that our study showed the possibility that the traditional paradigm of body MRI can be changed using GRASP. Adopting GRASP in routine clinical imaging may alter the current clinical practice in terms of handling undiagnostic dynamic T1WI. First, GRASP allows continuous scanning, obviating the need for bolus-tracking, a test bolus, or a fixed time delay for capturing the arterial window. Second, we were able to obtain consistently acceptable images in all patients using a gated reconstruction with a temporal resolution of 13.3 seconds, despite transient motion. This approach can lead to an improved workflow by reducing cases of re-examination, thereby alleviating the additional burden to radiologists and radiology technicians, and ultimately saving patients from unnecessary procedures. Furthermore, this technique would open the door to patients with limited breath-hold capacity allowing full investigation of their condition. Indeed, in our study, patients who had short breathing capacity (≤10 seconds) were also able to achieve acceptable image quality.

As for the dynamic phases, we compared the diagnostic performances of nongated and gated GRASP using different temporal resolutions. We found that the gated 6-second GRASP showed better diagnostic performance in detecting FLLs than the nongated 13.3-second GRASP. As discussed earlier, this difference may stem from the removal of motion artifacts after gating. In addition, the shorter temporal resolution may also help to visualize more subtle enhancement characteristics in the early dynamic phase and contribute to improved diagnostic performance. A shorter temporal resolution would be able to depict the hemodynamic changes of FLLs in greater detail and overcome this issue of temporal blurring. However, it must be noted that a decreasing number of radial spokes per image can increase streak artifacts and increase susceptibility to motion as well as lower signal-to-noise ratio.[12,32] Thus, there still remains a question as to the appropriate clinical temporal resolution for balancing image quality and diagnostic performance on the dynamic phase. Likewise, tweaking the regularization weight for the reconstruction, which was

TABLE 4. JAFROC FOM and 95% CI for Fixed Reader and Random Case Analysis

Sequence	FOM Values (95% CI)	*P*		
Free-breathing dynamic T1WI		A vs B	A vs C	B vs C
Nongated 13.3-s T1WI (A)	0.60 (0.56–0.65)	0.24	0.004	0.12
Respiratory gated 13.3-s T1WI (B)	0.64 (0.57–0.72)			
Respiratory gated 6-s T1WI (C)	0.69 (0.63–0.76)			

JAFROC indicates jackknife alternative free-response receiver operating characteristic; FOM, figure of merit; CI, confidence interval.

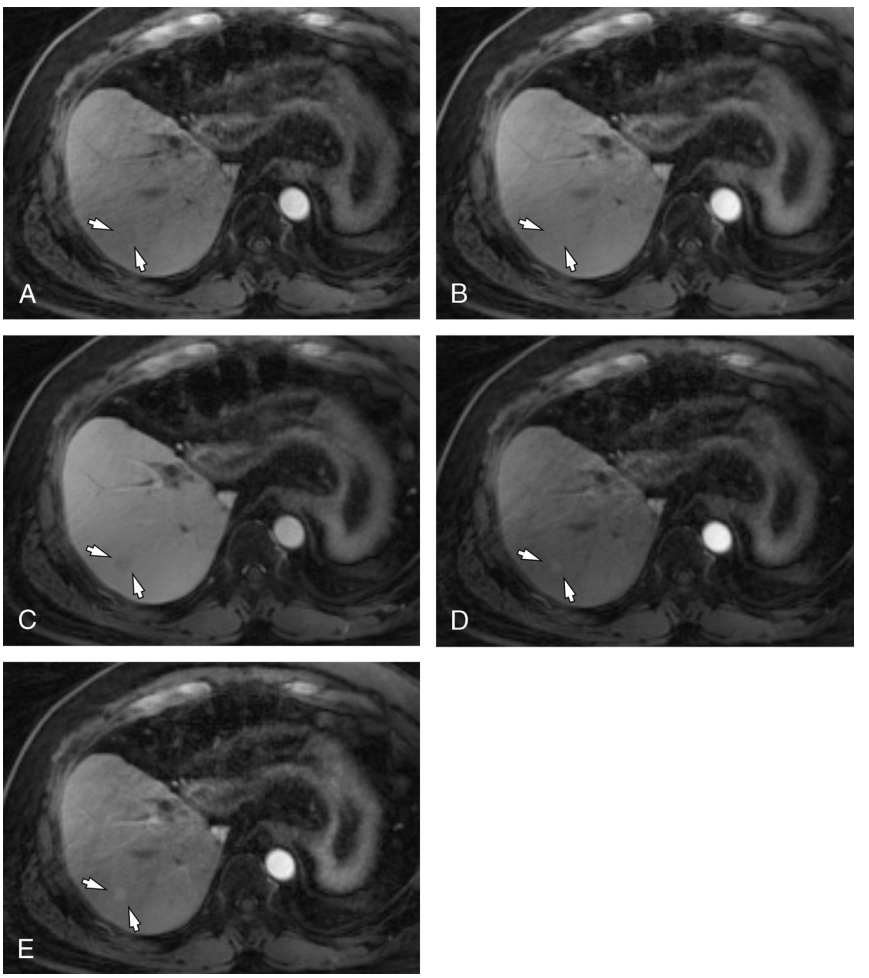

FIGURE 4. Feasibility of flexible time resolution of free-breathing T1WI using GRASP in a 53-year-old man who received a living-donor liver transplantation. On early arterial (A), late arterial (B), and portal venous phases (C) of gated T1WI with a 13.3-second time resolution, a 1.1-cm nonhypervascular nodule was found in S7 (arrows). On gated T1WI using a 6-second time resolution, arterial enhancement of the nodule was captured (arrows) on early and late arterial phases (D and E).

chosen empirically in this study, could be used to balance between strong suppression of undersampling artifacts and optimal temporal resolution. Because GRASP allows retrospective reconstruction, further studies are warranted so as to determine the optimal temporal resolution for the initial evaluation and secondary imaging interpretation in daily practice.

Our study has several limitations. First, the number of recruited patients in our prospective study was relatively small. Second, we defined transient motion based on respiratory frequency. Although we believe that alteration of amplitude alone without changes in frequency would rarely occur, we may have ignored the effect of amplitude. In addition, we only observed motion after contrast media or saline injection in a free-breathing state, so the causal relationship between contrast media administration and motion should be interpreted cautiously. Fourth, there would be a concern that bias could be caused by our notification of saline or contrast medium is about to be injected. However, we did not specify which would be injected into the patients, and setting of administration was the same to minimize any potential bias. In addition, we believe that more bias could be brought by an unpredicted, unnotified event, if we did not notice it to the patients, which is the reason why we inform the patients in a clinical practice. Fifth, we did not compare free-breathing T1WI using GRASP with conventional breath-hold T1WI for the dynamic phase as our study population underwent liver MRI for clinical purposes, and side-by-side comparison would not have been possible. However, we believe that the advantage of this technique is to provide clinically acceptable image quality consistently. Finally, motion artifacts were not completely eliminated when gating was applied. Thus, there are still concerns over the application of free-breathing T1WI in patients with sufficient breath-holding capacity. However, a transient motion was often observed in our study, and it is not easy to predict whether the motion would occur or not, and how significantly the arterial phase would be affected. Thus, we believe that there is still benefit in consistently obtaining the dynamic phase in most patients.

In conclusion, transient motion developed in 40% (23/59) of the study patients shortly after gadoxetic acid administration, and gated free-breathing T1WI using GRASP was able to consistently provide acceptable arterial phase imaging even in patients with transient motion.

ACKNOWLEDGMENTS

The authors thank Chris Woo for his editorial assistance.

REFERENCES

1. Lee KH, Lee JM, Park JH, et al. MR imaging in patients with suspected liver metastases: value of liver-specific contrast agent gadoxetic acid. *Korean J Radiol*. 2013;14:894–904.

2. Lee YJ, Lee JM, Lee JS, et al. Hepatocellular carcinoma: diagnostic performance of multidetector CT and MR imaging-a systematic review and meta-analysis. *Radiology*. 2015;275:97–109.
3. Deshmane A, Gulani V, Griswold MA, et al. Parallel MR imaging. *J Magn Reson Imaging*. 2012;36:55–72.
4. Yoo JL, Lee CH, Park YS, et al. The short breath-hold technique, controlled aliasing in parallel imaging results in higher acceleration, can be the first step to overcoming a degraded hepatic arterial phase in liver magnetic resonance imaging: a prospective randomized control study. *Invest Radiol*. 2016;51:440–446.
5. Davenport MS, Caoili EM, Kaza RK, et al. Matched within-patient cohort study of transient arterial phase respiratory motion-related artifact in MR imaging of the liver: gadoxetate disodium versus gadobenate dimeglumine. *Radiology*. 2014;272:123–131.
6. Davenport MS, Viglianti BL, Al-Hawary MM, et al. Comparison of acute transient dyspnea after intravenous administration of gadoxetate disodium and gadobenate dimeglumine: effect on arterial phase image quality. *Radiology*. 2013;266:452–461.
7. Luetkens JA, Kupczyk PA, Doerner J, et al. Respiratory motion artefacts in dynamic liver MRI: a comparison using gadoxetate disodium and gadobutrol. *Eur Radiol*. 2015;25:3207–3213.
8. Pietryga JA, Burke LM, Marin D, et al. Respiratory motion artifact affecting hepatic arterial phase imaging with gadoxetate disodium: examination recovery with a multiple arterial phase acquisition. *Radiology*. 2014;271:426–434.
9. Motosugi U, Bannas P, Bookwalter CA, et al. An investigation of transient severe motion related to gadoxetic acid-enhanced MR imaging. *Radiology*. 2016;279:93–102.
10. McClellan TR, Motosugi U, Middleton MS, et al. Intravenous gadoxetate disodium administration reduces breath-holding capacity in the hepatic arterial phase: a multi-center randomized placebo-controlled trial. *Radiology*. 2016;282:361–368.
11. Feng L, Grimm R, Block KT, et al. Golden-angle radial sparse parallel MRI: combination of compressed sensing, parallel imaging, and golden-angle radial sampling for fast and flexible dynamic volumetric MRI. *Magn Reson Med*. 2014;72:707–717.
12. Chandarana H, Feng L, Block TK, et al. Free-breathing contrast-enhanced multiphase MRI of the liver using a combination of compressed sensing, parallel imaging, and golden-angle radial sampling. *Invest Radiol*. 2013;48:10–16.
13. Feng L, Benkert T, Block KT, et al. Compressed sensing for body MRI. *J Magn Reson Imaging*. 2017;45:966–987.
14. Grimm R, Nickel MD, Wang Q. *Motion-Robust Abdominal DCE-MRI Using Respiratory-Gated Golden-Angle Radial Sparse Parallel MRI*. Singapore: ISMRM; 2016.
15. Grimm R, Feng L, Forman C. *Automatic Bolus Analysis for DCE-MRI Using Radial Golden-Angle Stack-of-stars GRE Imaging*. Melbourne, Australia: ISMRM; 2013.
16. Mortele KJ, Ros PR. Cystic focal liver lesions in the adult: differential CT and MR imaging features. *Radiographics*. 2001;21:895–910.
17. Goshima S, Kanematsu M, Watanabe H, et al. Hepatic hemangioma and metastasis: differentiation with gadoxetate disodium-enhanced 3-T MRI. *AJR Am J Roentgenol*. 2010;195:941–946.
18. Grieser C, Steffen IG, Seehofer D, et al. Histopathologically confirmed focal nodular hyperplasia of the liver: gadoxetic acid-enhanced MRI characteristics. *Magn Reson Imaging*. 2013;31:755–760.
19. Choi JY, Lee JM, Sirlin CB. CT and MR imaging diagnosis and staging of hepatocellular carcinoma: part II. Extracellular agents, hepatobiliary agents, and ancillary imaging features. *Radiology*. 2014;273:30–50.
20. Choi JY, Lee JM, Sirlin CB. CT and MR imaging diagnosis and staging of hepatocellular carcinoma: part I. Development, growth, and spread: key pathologic and imaging aspects. *Radiology*. 2014;272:635–654.
21. Hope TA, Fowler KJ, Sirlin CB, et al. Hepatobiliary agents and their role in LI-RADS. *Abdom Imaging*. 2015;40:613–625.
22. Mitchell DG, Bruix J, Sherman M, et al. LI-RADS (Liver Imaging Reporting and Data System): summary, discussion, and consensus of the LI-RADS Management Working Group and future directions. *Hepatology*. 2015;61:1056–1065.
23. Hallgren KA. Computing inter-rater reliability for observational data: an overview and tutorial. *Tutor Quant Methods Psychol*. 2012;8:23–34.
24. Chakraborty DP. Analysis of location specific observer performance data: validated extensions of the jackknife free-response (JAFROC) method. *Acad Radiol*. 2006;13:1187–1193.
25. Chakraborty DP. Validation and statistical power comparison of methods for analyzing free-response observer performance studies. *Acad Radiol*. 2008;15:1554–1566.
26. Park YS, Lee CH, Kim IS, et al. Usefulness of controlled aliasing in parallel imaging results in higher acceleration in gadoxetic acid-enhanced liver magnetic resonance imaging to clarify the hepatic arterial phase. *Invest Radiol*. 2014;49:183–188.
27. Bashir MR, Castelli P, Davenport MS, et al. Respiratory motion artifact affecting hepatic arterial phase MR imaging with gadoxetate disodium is more common in patients with a prior episode of arterial phase motion associated with gadoxetate disodium. *Radiology*. 2015;274:141–148.
28. Kim SY, Park SH, Wu EH, et al. Transient respiratory motion artifact during arterial phase MRI with gadoxetate disodium: risk factor analyses. *AJR Am J Roentgenol*. 2015;204:1220–1227.
29. Heyn C, Sue-Chue-Lam D, Jhaveri K, et al. MRI of the pancreas: problem solving tool. *J Magn Reson Imaging*. 2012;36:1037–1051.
30. Yoon JH, Lee JM, Yu MH, et al. Triple arterial phase MR imaging with gadoxetic acid using a combination of contrast enhanced time robust angiography, keyhole, and viewsharing techniques and two-dimensional parallel imaging in comparison with conventional single arterial phase. *Korean J Radiol*. 2016;17:522–532.
31. Nishimura DG, Jackson JI, Pauly JM. On the nature and reduction of the displacement artifact in flow images. *Magn Reson Med*. 1991;22:481–492.
32. Chandarana H, Block TK, Rosenkrantz AB, et al. Free-breathing radial 3D fat-suppressed T1-weighted gradient echo sequence: a viable alternative for contrast-enhanced liver imaging in patients unable to suspend respiration. *Invest Radiol*. 2011;46:648–653.
33. Chandarana H, Feng L, Ream J, et al. Respiratory motion-resolved compressed sensing reconstruction of free-breathing radial acquisition for dynamic liver magnetic resonance imaging. *Invest Radiol*. 2015;50:749–756.
34. Yoon JH, Yu MH, Chang W, et al. Clinical feasibility of free-breathing dynamic T1-weighted imaging with gadoxetic acid-enhanced liver magnetic resonance imaging using a combination of variable density sampling and compressed sensing. *Invest Radiol*. 2017; doi: 10.1097/RLI.0000000000000385.
35. Kaltenbach B, Bucher AM, Wichmann JL, et al. Dynamic liver magnetic resonance imaging in free-breathing: feasibility of a cartesian T1-weighted acquisition technique with compressed sensing and additional self-navigation signal for hard-gated and motion-resolved reconstruction. *Invest Radiol*. 2017; doi:10.1097/RLI.0000000000000396.
36. Hope TA, Saranathan M, Petkovska I, et al. Improvement of gadoxetate arterial phase capture with a high spatio-temporal resolution multiphase three-dimensional SPGR-Dixon sequence. *J Magn Reson Imaging*. 2013;38:938–945.